Vol 15 No 10, October 2006
1009-1963/2006/15(10)/2275-13
Chinese Physics
© 2006 Chin. Phys. Soc.
and IOP Publishing Ltd

Laser controlled quantum motion of two Paul trapped ions*

Cai Li-Hua(蔡丽华), Hai Wen-Hua(海文华)†, and Lu Geng-Biao(鲁耿彪)

Department of Physics, Hunan Normal University, Changesha 410081, *China*

(Received 26 February 2006; revised manuscript received 31 March 2006)

We investigate the quantum motion of two ions stored in a Paul trap and interacting with a time-periodic laser field. In the pseudopotential approximation and large detuning condition, we find that the relative motion is independent of the laser field, but the exact centre-of-mass motion is closely related to the laser field. By adjusting the laser intensity and frequency, we can well control the quantum motion of the centre-of-mass. We illustrate some physical properties described by the centre-of-mass states, such as the squeezed coherent property, the widths and heights of the wavepackets of probability density, the classical-quantum correspondence, the resonance ladders of expectation energy and the transition probabilities between time-dependent quantum levels.

Keywords: Paul trap, quantum wavepacket, energy ladder, laser control
PACC: 3280P, 0365G, 0340K

1. Introduction

The Paul trap has been applied in many fields of science and technology.[1] Especially, in recent years, the Paul trap as a powerful tool has been extensively used in the investigations of quantum logic operations,[2,3] quantum computation,[4−6] quantum information,[7−9] and the state preparations.[10−13] The interaction of a trapped ion with the laser beam has received much attention.[14−23] When the laser intensity is small, the effect of the laser can be treated as a perturbation to the system. With the increase of the intensity, the motion becomes more and more complex, so we must seek new methods to solve it. The Green function method was applied to treating the quantum transition of a harmonically trapped particle in a strong external field.[14] In the Lamb–Dicke limit and rotating wave approximation, Jiang *et al*[22] have investigated the dynamics of a trapped ultra-cold ion in the standing-wave laser with a time-dependent external potential. Qu and co-workers[23] have illustrated the interaction between a trapped ion with a single-mode quantized radiation field. Due to the loss of validity of the perturbation technique, it is very important to obtain a set of exact solutions[15−18] for the considered systems. The two trapped ions interacting with the laser beam has also aroused much interest.[24−30] Munro *et al*[24] have described how entangled qubits can be encoded as entangled coherent states of two-dimensional centre-of-mass vibrational motion for two ions in an ion trap. Feng *et al* gave some series solutions of two trapped ions.[25,26] Solano *et al*[27] made the rotating-wave approximation (RWA) with respect to the vibrational frequencies to obtain the interaction Hamiltonian. Yin *et al*[28] used the split-operator method to analyse the energies and the eigenstates of the two trapped ions. Li *et al*[29] discussed the controlling rotation (CROT) operation to handle the two laser beams with different intensities, which illuminate two different ions in a harmonic trap for studying the quantum logic gate operation between different ions in a trap. They found that under certain conditions, the interaction could realize a universal two-qubit operation.

In this paper, we consider a one-dimensional system of two trapped ions interacting with a time-periodic strong laser field.[31−33] In the pseudopotential approximation and large detuning condition, by using the variable-separation technique and test-function method,[15−36] we obtain n exact solutions of the relative motion and the centre-of-mass motion. Through theoretical analysis and numerical calculations, we find the relative motion to be independent of the external field. We demonstrate some interesting

*Project supported by the National Natural Science Foundation of China (Grant Nos 10575034 and 10275023), and the Science Foundation of the Laboratory of Magnetic Resonance and Atomic and Molecular Physics, China (Grant No T152504).
†Corresponding author, E-mail: adcve@public.cs.hn.cn

physical properties of the centre-of-mass motion, such as the generalized squeezed coherent states, classical-quantum correspondence, resonance ladders of the expectation energies, quantum transitions, and the control of the probability wave-packet-trains.

The rest of this article is organized as follows. In Section 2, we construct the exact solution of a quantum system and analyse the squeezed coherent property of the exact state. In Section 3, we investigate the quantum transitions and resonance ladders of the expectation energy via the exact solutions of the centre-of-mass motion. In Section 4, we discuss how to realize the control of wave-packet-train by adjusting an external field. Finally, in Section 5, we make some concluding remarks.

2. Exact solution of the system

We investigate the exact solution of a time-dependent one-dimensional system that is associated with two Paul-trapped ions interacting with an external laser field. In the pseudopotential approximation and large detuning condition, the Hamiltonian governing this system reads[5]

$$H = \frac{p_1^2}{2m} + \frac{p_2^2}{2m} + V(x_1) + V(x_2) + \frac{e^2}{4\pi\epsilon_0|x_2 - x_1|} + \varepsilon(x_1 + x_2)\cos\omega t, \quad (1)$$

where $V(x_i)$ denotes the confining potentials along the x-axis, which is symmetric, $V(x_i) = V(-x_i)$, the final term on the right-hand side of Eq.(1) is the time-dependent linear potential generated by a strong laser[31,32] with ε and ω respectively being the strength and frequency of laser, where the Kramers–Henneberger transformation has been employed.[34,35] We denote by x_e the separation between the ions at the equilibrium position. Using the centre-of-mass and relative coordinates, $x_c = (x_1 + x_2)/2$, $x_r = x_2 - x_1 - x_e$, $p_c = p_1 + p_2$, and $p_r = (p_2 - p_1)/2$, and expanding around the equilibrium position $x_c = x_r = 0$ up to the second order,[5] we obtain the Hamiltonian operator

$$\hat{H} = -\frac{\hbar^2}{2m_c}\frac{\partial^2}{\partial x_c^2} - \frac{\hbar^2}{2m_r}\frac{\partial^2}{\partial x_r^2} + \frac{1}{2}m_c\omega_c^2 x_c^2 + \frac{1}{2}m_r\omega_r^2 x_r^2 + 2\varepsilon x_c\cos\omega t. \quad (2)$$

Here $m_c = 2m$, $m_r = m/2$, $\omega_{c,r}$ are the corresponding frequencies in the harmonic approximation,[5] $\omega_c^2 = \frac{1}{m_c}\frac{\partial^2 V}{\partial x_c^2}|_{eq}$, and $\omega_r^2 = \omega_c^2 + \frac{e^2}{\pi\epsilon_0 m x_e^3}$.

The motion of the ions is dominated by the time-dependent Schrödinger equation

$$i\hbar\frac{\partial\psi}{\partial t} = -\frac{\hbar^2}{2m_c}\frac{\partial^2\psi}{\partial x_c^2} - \frac{\hbar^2}{2m_r}\frac{\partial^2\psi}{\partial x_r^2} + \frac{1}{2}m_c\omega_c^2 x_c^2\psi + \frac{1}{2}m_r\omega_r^2 x_r^2\psi + 2\varepsilon x_c\cos\omega t\psi. \quad (3)$$

As the trap potential is independent of time, we can assume the relative wavefunction to be of stationary state, which implies

$$\psi(x_c, x_r, t) = \psi_c(x_c, t)\psi_r(x_r)e^{-i\frac{E_r}{\hbar}t}, \quad (4)$$

where ψ_c, ψ_r and E_r are called the centre-of-mass wavefunction, relative wavefunction and relative energy respectively. Applying them to Eq.(3) yields

$$\frac{1}{\psi_c}i\hbar\frac{\partial\psi_c}{\partial t} + \frac{1}{\psi_c}\frac{\hbar^2}{2m_c}\frac{\partial^2\psi_c}{\partial x_c^2} - \frac{1}{2}m_c\omega_c^2 x_c^2 - 2\varepsilon x_c\cos\omega t = -\frac{1}{\psi_r}\frac{\hbar^2}{2m_r}\frac{\partial^2\psi_r}{\partial x_r^2} + \frac{1}{2}m_r\omega_r^2 x_r^2 - E_r. \quad (5)$$

The left side of this equation is only related to x_c and t, and the right side is only dependent on x_r, while x_c, x_r and t are all independent variables. So in the equation, both the left side and right side are equated to the same constant, where we assume the constant to be zero, thus Eq.(5) can be separated into the following two equations:

$$i\hbar\frac{\partial\psi_c}{\partial t} = -\frac{\hbar^2}{2m_c}\frac{\partial^2\psi_c}{\partial x_c^2} + \frac{1}{2}m_c\omega_c^2 x_c^2\psi_c + 2\varepsilon x_c\cos\omega t\psi_c, \quad (6)$$

$$E_r\psi_r = -\frac{\hbar^2}{2m_r}\frac{\partial^2\psi_r}{\partial x_r^2} + \frac{1}{2}m_r\omega_r^2 x_r^2\psi_r. \quad (7)$$

The relative motion governed by Eq.(7) is of a one-dimensional linear harmonic oscillator, from the elementary quantum mechanics we can obtain the wavefunction[37]

$$\psi_r(x_r) = \left(\frac{1}{\sqrt{\pi}2^n n!}\right)^{1/2} e^{-\frac{1}{2}l_r^2 x_r^2} H_n(l_r x_r), \quad (8)$$

where $l_r = \sqrt{\frac{\hbar}{m_r\omega_r}}$. We do not discuss more about this well known solution, since it is independent of the external laser field, but we pay our attention to the centre-of-mass motion.

For simplicity, we first transform Eq.(6) into the dimensionless form

$$i\frac{\partial\psi_c}{\partial t} = -\frac{1}{2}\frac{\partial^2\psi_c}{\partial x_c^2} + \frac{1}{2}x_c^2\psi_c + \varepsilon_0 x_c\cos\Omega t\psi_c. \quad (9)$$

Here we have adopted the natural units with $m_c = \hbar = \omega_c = 1$ so that the space-time coordinates x_c and t are respectively in units of the harmonic oscillator length $l_c = \sqrt{\hbar/(m_c\omega_c)}$ and inverse frequency ω_c^{-1}. The laser frequency is normalized by ω_c, and the laser intensity becomes $\varepsilon_0 = \sqrt{\frac{4}{m_c\hbar\omega_c^3}}\varepsilon$. Applying the well-known technique to solving the time-dependent Schrödinger equation,[15] we construct the n exact solutions of Eq.(9) as (see the Appendix)

$$\begin{aligned}&\psi_c = \Psi_n(x_c,t) = R_n(x_c,t)\exp[\mathrm{i}\Theta_n(x_c,t)],\\ &n = 0,1,2,\ldots,\end{aligned} \tag{10}$$

where the real function $R_n(x_c,t)$ and $\Theta_n(x_c,t)$ read

$$\begin{aligned}R_n(x_c,t) =&\left[\frac{\sqrt{c_0}}{\sqrt{\pi}2^n n!\rho(t)}\right]^{1/2} H_n(\xi)\exp\left(-\frac{1}{2}\xi^2\right),\\ \Theta_n(x_c,t) =&\frac{\dot\rho(t)}{2\rho(t)}x_c^2 + b''(t)x_c\\ &+\int\left[\frac{b'^2(t)}{2} - \frac{b''^2(t)}{2}\right]\mathrm{d}t - \left(\frac{1}{2}+n\right)\theta(t),\\ \xi(x_c,t) =&\frac{\sqrt{c_0}x_c}{\rho(t)} - \frac{b'(t)\rho(t)}{\sqrt{c_0}}.\end{aligned} \tag{11}$$

In Eq.(11), $\sqrt{c_0}$ is an integration constant, $\rho(t)$ and $\theta(t)$, $b'(t)$ and $b''(t)$ are real functions in the following forms:

$$\begin{aligned}\rho(t) =&\sqrt{A^2\cos^2(t+\alpha) + B^2\cos^2(t+\beta)},\\ \theta(t) =&\arctan\frac{B\cos(t+\beta)}{A\cos(t+\alpha)},\\ b'(t) =&\frac{b_0''\sin\theta}{\rho} + \frac{b_0'\cos\theta}{\rho}\\ &-\frac{\varepsilon_0\sin\theta}{\rho}\int\cos\Omega t\rho\cos\theta\mathrm{d}t\\ &+\frac{\varepsilon_0\cos\theta}{\rho}\int\cos\Omega t\rho\sin\theta\mathrm{d}t,\\ b''(t) =&\frac{b_0''\cos\theta}{\rho} - \frac{b_0'\sin\theta}{\rho}\\ &-\frac{\varepsilon_0\cos\theta}{\rho}\int\cos\Omega t\rho\cos\theta\mathrm{d}t\\ &-\frac{\varepsilon_0\sin\theta}{\rho}\int\cos\Omega t\rho\sin\theta\mathrm{d}t,\end{aligned} \tag{12}$$

where A, B, b_0', b_0'', α and β are some real constants associated with initial conditions. It is noticeable that there exist the relations between ρ and θ: $\rho\cos\theta = A\cos(t+\alpha)$, and $\rho\sin\theta = B\cos(t+\beta)$.

The module $R_n(x_c,t)$ of the exact solution for any quantum number n describes the wavepacket train consisting of $n+1$ packets. When the system parameters are taken as the values in a wide range, we can obtain some different kinds of quantum states, which can be used to treat various physical problems. For example, take $A = B = \sqrt{c_0}$, $\alpha = 0$ and $\beta = -\frac{\pi}{2}$, and we will have $\xi = x - b'(t)$, the corresponding ground state with $n = 0$ being the result reported in Ref.[16]. Because of the property of the orthonormalization, the solution of Eq.(10) can serve as a complete basis to investigate more physical systems; say the Bose–Einstein condensate held in the harmonic potential.[36] The function $\rho(t)$ in Eq.(11) can be called the function of width and height of the wave-packet-train.[36] Taking $\alpha = 0$, $\beta = -\pi/2$ and $A = B$, $\rho(t)$ will be a constant, which means that in a particular case the width and height of wave-packet-tain do not change with time. In other cases, the function $\rho(t)$ periodically varies with time, causing the corresponding changes in width and height of wave-packet-train, which are identified with the so-called breathing and oscillation of wave-packets.[38] The orbit of the centre of the wavepacket train $x_c(x,t)$ is given by ξ=0. Using Eqs.(11) and (12), from ξ=0 we have the orbit

$$\begin{aligned}x_0(t) =&\frac{\rho^2(t)}{c_0}b' = c_0^{-1}b_0'A\cos(t+\alpha)\\ &+c_0^{-1}b_0''B\cos(t+\beta)\\ &+\varepsilon_0 AB\cos(t+\alpha)\int\cos\Omega t\cos(t+\beta)\mathrm{d}t\\ &-\varepsilon_0 AB\cos(t+\beta)\int\cos\Omega t\cos(t+\alpha)\mathrm{d}t.\end{aligned} \tag{13}$$

This is just the classical orbit of the driven harmonic oscillator governed by $\ddot x_c = -x_c + \varepsilon_0\cos\Omega t$. Equation (13) indicates that the centre of wave-packet-train oscillates periodically like a classical harmonic oscillator.

Making use of the orthonormalization condition $\langle\Psi_n|\Psi_{n'}\rangle = \delta_{nn'}$ and the formulae

$$\begin{aligned}\xi =&e(t)x - f(t),\\ \xi\Psi_n =&\sqrt{n/2}\,\Psi_{n-1}\mathrm{e}^{-\mathrm{i}\theta} + \sqrt{(n+1)/2}\,\Psi_{n+1}\mathrm{e}^{\mathrm{i}\theta},\\ 2\xi^2\Psi_n =&\sqrt{n(n-1)}\,\Psi_{n-2}\mathrm{e}^{-2\mathrm{i}\theta} + (2n+1)\Psi_n\\ &+\sqrt{(n+1)(n+2)}\,\Psi_{n+2}\mathrm{e}^{2\mathrm{i}\theta},\\ \frac{1}{H_n}\frac{\partial H_n}{\partial\xi}\Psi_n =&2n\frac{H_{n-1}}{H_n}\Psi_n = \sqrt{2n}\,\Psi_{n-1}\mathrm{e}^{-\mathrm{i}\theta},\end{aligned} \tag{14}$$

we calculate the expectation values of coordinate x_c

and the momentum $p_{\rm c}$ as[36]

$$\begin{aligned}
\overline{x}_{\rm c} =&\langle\,\Psi_n|x_{\rm c}|\,\Psi_n\rangle = \frac{\rho^2}{c_0}b' = x_0,\\
\overline{p}_{\rm c} =&\langle\,\Psi_n|-{\rm i}\frac{\partial}{\partial x_{\rm c}}|\,\Psi_n\rangle = b'' + \frac{\dot\rho}{\rho}\overline{x}_{\rm c} = \dot{\overline{x}}_{\rm c},\\
\overline{x_{\rm c}^2} =&\langle\,\Psi_n\mid \hat{x_{\rm c}^2}\mid\,\Psi_n\rangle\\
=&c_0^{-1}\rho^2(t)\left[n+\frac{1}{2}+\frac{\rho^2(t)b'^2(t)}{c_0}\right],\\
\overline{p_{\rm c}^2} =&\langle\,\Psi_n\mid \hat{p_{\rm c}^2}\mid\,\Psi_n\rangle\\
=&\left[\frac{\dot\rho^2(t)}{c_0}+\frac{c_0}{\rho^2(t)}\right]\left(n+\frac{1}{2}\right)+b''^2(t)\\
&+\frac{b'^2(t)\dot\rho^2(t)\rho^2(t)}{c_0^2}+\frac{2b'(t)b''(t)\dot\rho(t)\rho(t)}{c_0}.
\end{aligned}\tag{15}$$

Interestingly, we find that the expectation value of position in Eq.(15) is equal to the centre coordinate of wave-packet-train in Eq.(13), and the expectation momentum is its time derivative. Therefore, the expectation 'quantum orbit' agrees with the corresponding classical orbit, which demonstrates a good classical-quantum correspondence.

From Eq.(15) we obtain the variations in position and momentum as

$$\begin{aligned}
\triangle x_{\rm c}(t) =&(\overline{x_{\rm c}^2}-\overline{x}_{\rm c}^2)^{1/2} = \frac{\rho(t)}{\sqrt{c_0}}\sqrt{n+\frac{1}{2}},\\
\triangle p_{\rm c}(t) =&(\overline{p_{\rm c}^2}-\overline{p}_{\rm c}^2)^{1/2}\\
=&\sqrt{\left[\frac{\dot\rho^2(t)}{c_0}+\frac{c_0}{\rho^2(t)}\right]}\sqrt{n+\frac{1}{2}}.
\end{aligned}\tag{16}$$

It is well known[37] that for the dimensionless $x_{\rm c}$ and $p_{\rm c}$ the energy eigenstates of a harmonic oscillator are associated with $\triangle x_{\rm c} = \triangle p_{\rm c} = \sqrt{n+\frac{1}{2}}$, and in a coherent state of harmonic oscillator we have $\triangle x_{\rm c} = \triangle p_{\rm c} = \frac{1}{\sqrt{2}}$. From Eq.(16), we find that in the exact states in Eq.(10) of the driven harmonic oscillator the $\triangle x_{\rm c}$ and $\triangle p_{\rm c}$ vary with time. However, they are independent of the time-dependent external field, since the function $\rho(t)$ governing their time evolutions does not depend on the external field. Note that a state is called the squeezed state[39] if the variations satisfy $\triangle x_{\rm c} < \frac{1}{\sqrt{2}}$ or $\triangle p_{\rm c} < \frac{1}{\sqrt{2}}$. Letting the squeezing parameter be $V_{\rm s}(t) = \sqrt{2}\triangle S(t)$ for $(S = x_{\rm c}, p_{\rm c})$, we determine the instantaneous squeezing states which obey $V_{\rm s}(t) < 1$ at some time t. The oscillating amplitude of $\rho(t)$ is determined by the parameters A and B, and the oscillating phase depends on the parameters α and β. Adjusting the system constants A, B, α, and β, we can obtain a series of interesting squeezed coherent states, and the squeezing parameters $V_{\rm s}$ periodically vary around 1 with different amplitudes and phases. For example, when taking $c_0 = 1, n = 0$ and $\rho = \sqrt{0.5\cos^2 t + 1.2\sin^2 t} = \sqrt{1.2 - 0.7\cos^2 t}$, Eq.(16) implies that $\triangle x_{\rm c}$ can vary between $\sqrt{1.2}\times\frac{1}{\sqrt{2}}$ and $\sqrt{0.5}\times\frac{1}{\sqrt{2}}$. Given Eq.(16), the Heisenberg uncertainty relation becomes

$$\begin{aligned}
\triangle x_{\rm c}(t)\,\triangle\, p_{\rm c}(t) =&\sqrt{\left[\frac{\dot\rho^2(t)\rho^2(t)}{c_0^2}+1\right]}\left(n+\frac{1}{2}\right)\\
\geq&\left(n+\frac{1}{2}\right).
\end{aligned}\tag{17}$$

This general relation contains the harmonic case $\triangle x_{\rm c}(t)\,\triangle\, p_{\rm c}(t) = (n+\frac{1}{2})$ for the constant ρ, with parameters $\alpha = 0, \beta = -\frac{\pi}{2}$, and $A = B$. When taking $n = 0$ and $\rho =$ constant, from Eq.(17) we arrive at the minimum uncertainty of the general coherent state, namely $\triangle x_{\rm c}(t)\,\triangle\, p_{\rm c}(t) = \frac{1}{2}$. The conclusion about the squeezed coherent state is similar to the result in Refs.[40,41].

Combining Eq.(14) with Eq.(15) and using the quantum-mechanical definition of average energy in the state Ψ_n, we arrive at

$$\begin{aligned}
E_n =&\langle\,\Psi_n|{\rm i}\frac{\partial}{\partial t}\,\Psi_n\rangle\\
=&\left(\frac{1}{2}+n\right)\frac{c_1}{c_0}+\frac{1}{2}[\overline{p}_{\rm c}^2+\overline{x}_{\rm c}^2]+\varepsilon_0\overline{x}_{\rm c}\cos\Omega t,
\end{aligned}\tag{18}$$

where $c_1 = (\dot\rho^2 + c_0^2/\rho^2 + \rho^2)/2$ is another integration constant. It is quite interesting that the time-dependent average energy in Eq.(18) is composed of classical and quantum parts with the final term being the contribution of external field, which is different from the expectation energy of the known coherent state. However, the external field does not affect the quantum part of the energy. From Eq.(18) we easily acquire the adjacent energy level spacing $\Delta E = E_{n+1} - E_n = \frac{c_1}{c_0}$, which is a constant determined by the integration constants c_1 and c_0. When we take the constants as $\alpha = 0, \beta = -\frac{\pi}{2}$, and $A = B = 1$, leading to $c_0 = c_1 = 1$, the quantum level becomes the well known level of the stationary state harmonic oscillator, $\Delta E = 1$ $(\hbar\omega)$. From the viewpoint of quantum mechanics, the ions can transit between the different quantum states, and this will be discussed in detail below.

3. Transition probabilities and energy ladders

For a weak laser field with small strength, the quantum transition can be treated approximately by using the quantum perturbation theory.[37] When the laser field is strong enough, we cannot use the traditional perturbation theory and must seek the effective nonperturbative methods, such as the Green's function method[14] and the exact-solution method. In fact, once the exact solutions are given, we can directly calculate the transition probabilities between the stationary states. To do so, we expand the exact quantum states $\Psi_n(x_c,t)$ by adopting the energy eigenstates of harmonic oscillator as

$$\Psi_n(x_c,t)=\sum_m C_{nm}(t)\psi_m(x_c). \tag{19}$$

As an example, we take the parameter set $\alpha=0,\beta=-\frac{\pi}{2}$, $A=B=c_0=1$, $b_0''=0$, $b'_{0,\Omega\neq1}=\frac{\varepsilon_0}{1-\Omega^2}$ and $b'_{0,\Omega=1}=\frac{\varepsilon_0}{2}$ so that Eq.(12) gives $\rho=1$, and $b'(0)=b''(0)=0$. And the initial state $\Psi_n(x_c,0)=\psi_n(x_c)$ is just the energy eigenstate of harmonic oscillator,

$$\psi_n(x_c)=N_nH_n(x_c)\exp\Big[-\frac{1}{2}x_c^2\Big], \tag{20}$$

where the x_c is dimensionless coordinate, $N_n=\left(\frac{1}{\sqrt{\pi}2^n n!}\right)^{1/2}$ is the normalization constant. Multiplying both sides of Eq.(19) by $\psi_{m'}(x_c)$, we integrate the resulting equation to yield the transition amplitude from state n to state m

$$C_{nm}(t)=\int_{-\infty}^{+\infty}\mathrm{d}x_c\psi_m^*(x_c)\,\Psi_n(x_c,t) \tag{21}$$

with the initial condition $C_{nm}(0)=\delta_{nm}$. In the computation, the orthnormalization condition, $\int_{-\infty}^{+\infty}\psi_{m'}(x_c)\psi_m(x_c)\mathrm{d}x_c=\delta_{m,m'}$, has been employed. The corresponding transition probability reads

$$P_{n,m}(t)=\mid C_{n,m}(t)\mid^2. \tag{22}$$

By applying the exact solution in Eq.(10) with the initial state $\Psi_n(x_c,0)=\psi_n(x_c)$ to Eqs.(21) and (22), we can exactly compute the transition probability $P_{n,m}(t)$ induced by the time-dependent laser field.

We now numerically illustrate the transition probability and average energy for the given parameters used previously. At first we are interested in the resonance case. Inserting such parameters and resonance frequency $\Omega=1(\omega)$ into Eqs.(10), (21) and (22), we have the time evolutions of transition probabilities as shown in Figs.1(a) and 1(b), where the external field strength is set as $\varepsilon_0=0.9$. In Fig.1(a) the transition probabilities $P_{0,1}(t)$ and $P_{0,4}(t)$ show that their peaks correspond to the time $t=\pi$ and $t=2\pi$ respectively, but plots of probabilities $P_{0,2}(t)$ and $P_{0,8}(t)$ indicate that the times associated with their peak values deviate from the integer times of π. In Fig.2(b), we show the transition probability $P_{1,3}(t)$ for a stronger laser field. The solid curve corresponds to $\varepsilon_0=60$ and the dotted curve to $\varepsilon_0=20$. All these plots show that the transition probabilities $P_{n,m}(t)$ tend to zero as $t\to\infty$. In particular, with the increase of the laser intensity, the curves are translated towards the left and the transition probabilities more early approach to zero. On the other hand, for the same parameters of Fig.1(a), Eqs.(12), (15) and (18) give $\rho^2=c_0=1$, $\overline{x}_c=b'(t)=\frac{1}{2}\varepsilon_0[\cos t-\cos^3 t-\sin t(t+\sin t\cos t)]$, $\overline{p}_c=\dot{\overline{x}}_c=-\frac{1}{2}\varepsilon_0(t\cos t+\sin t)$ and $E_n(t)=n+0.5+\varepsilon_0^2(0.0625+0.125t^2-0.0625\cos(2t)-0.125t\sin(2t))$. Based on these, we plot the time evolutions of average energies E_0, E_1 and E_6 for the external field strength $\varepsilon_0=0.9$ and resonance frequency $\Omega=1$ as shown in Fig.1(c). This figure shows that there exist some interesting plateaus of the energy curves, which are similar to the spatial ladders of the Wannier–Stark potential.[42] The centres of energy ladders are some inflexion points, which appear at $t=\pi k$ for $k=0,1,2,3,\ldots$, where $\dot{E}_n(t)=\frac{1}{4}\varepsilon_0^2t(1-\cos(2t))=0$ and $\ddot{E}_n(t)=0$. The resonance ladders of average energy result from the classical part of Eq.(18), however, the values of energy plateaus approximately satisfy the quantized relationship $E_n(t)=n+0.5+0.125\pi^2k^2\varepsilon_0^2$, for $k=1,2,3,\ldots$. From this formula, we can see that when the laser strength is set as $\varepsilon_0=\sqrt{8}/\pi\approx0.9$, the values of energy ladders obey $E_n(\pi k)=n+0.5+k^2$, which appear at $t=\pi k$ for $k=0,1,2,3,\ldots$. Simultaneously, the resonance leads the centre position in Eq.(13) of wavepacket train to infinity, indicating the lose of stability. The resonance lose of stability is therefore the reason for the transition from the initial state to any final state. These results approximately agree with the corresponding results obtained by the Green function method.[14] Although there may be some small differences between them, our results from the exact solution are more accurate. Particularly, a comparison between our exact results and those results from quantum perturbation theory shows that the selection rule[37] $\Omega-\omega=\pm1(\omega)$ of transitions is no longer valid for the strong field case.

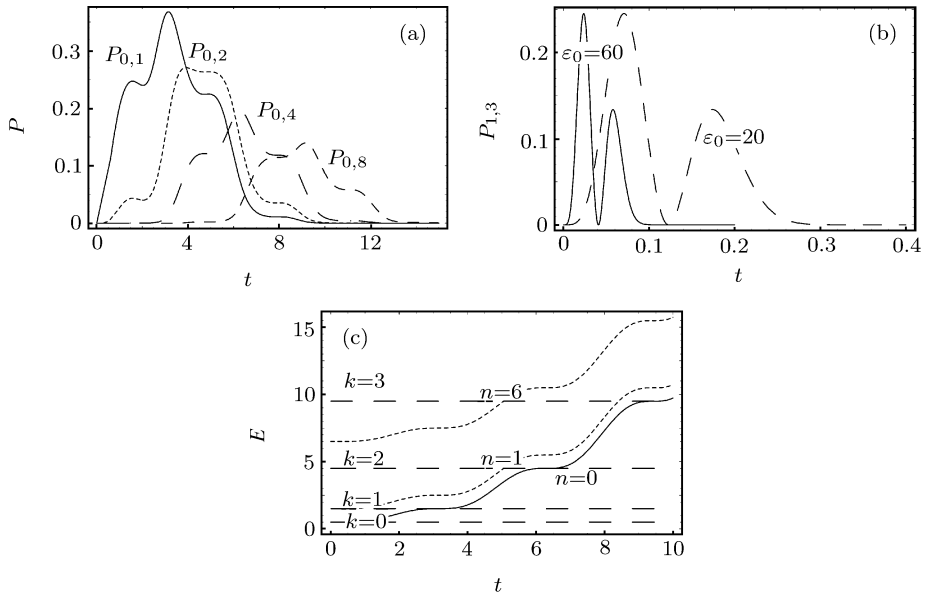


Fig.1. (a) The time evolutions of transition probabilities from Eqs.(10), (21) and (22) for the resonance case $\Omega = 1(\omega_c)$ with the laser strength $\varepsilon_0 = 0.9$. The solid lines expresses the probability $P_{0,1}(t)$ from $n = 0$ state to $m = 1$ state. The dotted line, middle-dashed and long-dashed lines represent $P_{0,2}(t)$, $P_{0,4}(t)$ and $P_{0,8}(t)$ respectively. (b) The transition probability $P_{1,2}(t)$ for two different values of laser strengths. The solid line is associated with $\varepsilon_0 = 60$, and the dotted line with $\varepsilon_0 = 20$. (c) The time evolution of average energy for the resonance case with parameters $\Omega = 1$, and $\varepsilon_0 = 0.9$. The solid line represents the average energy $E_0(t)$ of ground state, the dotted line denotes the average energy $E_1(t)$ and $E_6(t)$, and the long-dashed lines indicates the centres of energy ladders, $E_0(\pi k) = 0.5 + k^2$, which appear at $t = \pi k$ for $k = 0, 1, 2, 3, \ldots$. The space and time variables x and t are in units of l_c and ω_c^{-1} respectively.

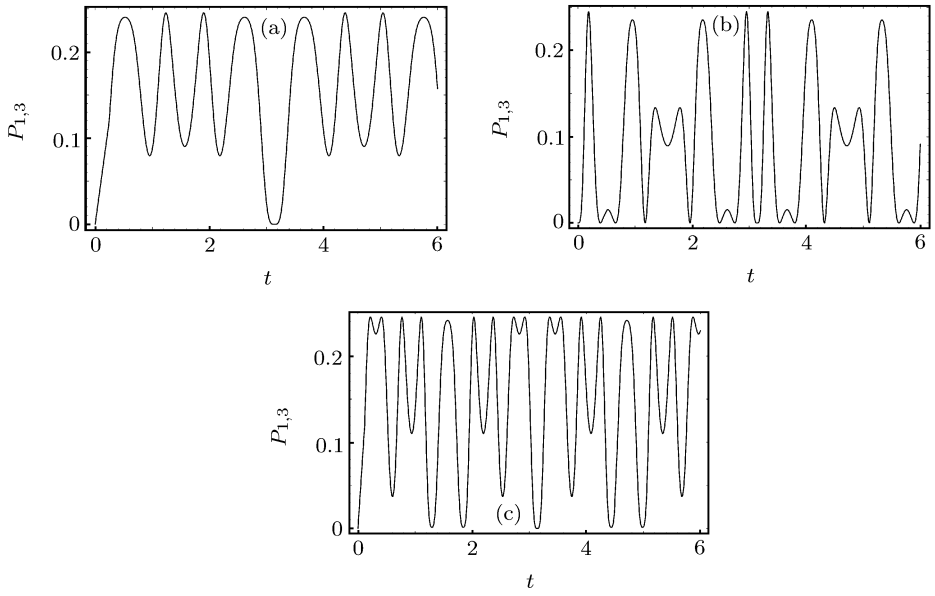


Fig.2. The time evolution of transition probability $P_{1,3}(t)$ in the non-resonance case for the parameters (a) $\Omega = 3$ and $\varepsilon_0 = 4$, (b) $\Omega = 3$ and $\varepsilon_0 = 8$, and (c)$\Omega = 5$ and $\varepsilon_0 = 8$. The same units as those in Fig.1 are used.

For the non-resonance case $\Omega \neq 1(\omega)$, we can also directly calculate the transition probabilities by using our exact solutions. Figure 2 shows the transition probabilities $P_{1,3}(t)$ for the different laser frequencies and amplitudes. The results for the non-resonance case indicate that the transition probability $P_{1,3}(t)$ periodically evolves and exists for all the time. For the larger laser strengths, the maxima of transition

probabilities can reach the values of the resonance peaks in Fig.1. A comparison between Fig.2(b) and Fig.2(c) displays that using the larger frequency difference $\Omega - \omega$ can produce more probability peaks.

It is interesting for us to analytically investigate the relationship between the transition probability and average energy. This relationship can be easily obtained by substituting the wavefunction of Eq.(9) into the formula of average energy,

$$\begin{aligned} E_n =& \langle \Psi_n(x_c, t) \mid \hat{H} \mid \Psi_n(x_c, t) \rangle \\ =& \sum_m \left(m + \frac{1}{2} \right) P_{n,m}(t) + \frac{\varepsilon_0 \cos(\Omega t)}{\sqrt{2}} \\ & \times \sum_m C_{n,m}(t) \sum_{m'} C_{n,m'}(t) (\sqrt{m'} \delta_{m,m'-1} \\ & + \sqrt{m'+1} \delta_{m,m'+1}), \end{aligned} \tag{23}$$

which differs from that of Eq.(18) in form. It exhibits the relationship between average energy and transition probability, which is more explicit than that of Eq.(18).

4. Laser control of the centre-of-mass motion

We have known that the function $\rho(t)$ describes the widths and heights of wavepacket trains and each packet of Eq.(11).[15] The widths and heights vary periodically with time, however, they are independent of the time-dependent external field. By taking the parameter set $A = 2$, $B = 1$, $\alpha = 0$ and $\beta = 0.01$, we can obtain the time evolution of $\rho(t)$ from Eq.(12) as shown in Fig.3.

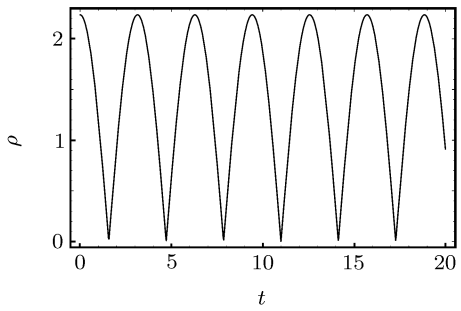


Fig.3. The time evolution of function $\rho(t)$ that exhibits the change period of the wavepacket's width and height to be π. The time t is in units of ω_c^{-1}.

In order to investigate the controlling of the centre-of-mass motion, we go back to the orbit of the wavepacket-train's centre. We can see from Eq.(13) that the centre motion can be controlled by adjusting the external field. For simplicity, taking the parameter set $b_0' = b_0'' = 0$, $\alpha = 0$, $\beta = -\pi/2$, A=B=1, $c_0 = 1$, $\rho = 1$, and $\theta = t$ and inserting them into Eq.(13), we can numerically plot the centre motion of wavepackets as shown in Fig.4 and Fig.5. First, we consider the resonance case $\Omega = 1(\omega)$, the numerical result is shown in Fig.4(a). We find that the centre orbit x_0 of wave-packet-train is very unstable because of the resonance, in which the oscillating amplitude becomes larger and larger. Obviously, the result will lead to the destabilization of quantum states and the occurrence of transition between different states. For the non-resonance case as indicated in Fig.4(b) and 4(c), we find that the centre orbit x_0 oscillates periodically with time. A comparison between curves in Figs.4(b) and 4(c) exhibits that the high frequency can lead to the stabilization of the wave-packet-train. However, from Figs.5(a), 5(b) and 5(c), we can find that with the increase of the laser strength ε_0, the amplitude of centre of wave-packet-train becomes larger and larger, which means that the strong laser field may lead to an instability of the wave-packet-train. From the above numerical analysis, we know that by adjusting the external field parameters (Ω and ε_0) we can effectively control the centre of wave-packet-train theoretically, including the position of centre and the stability of wave-packet-train.

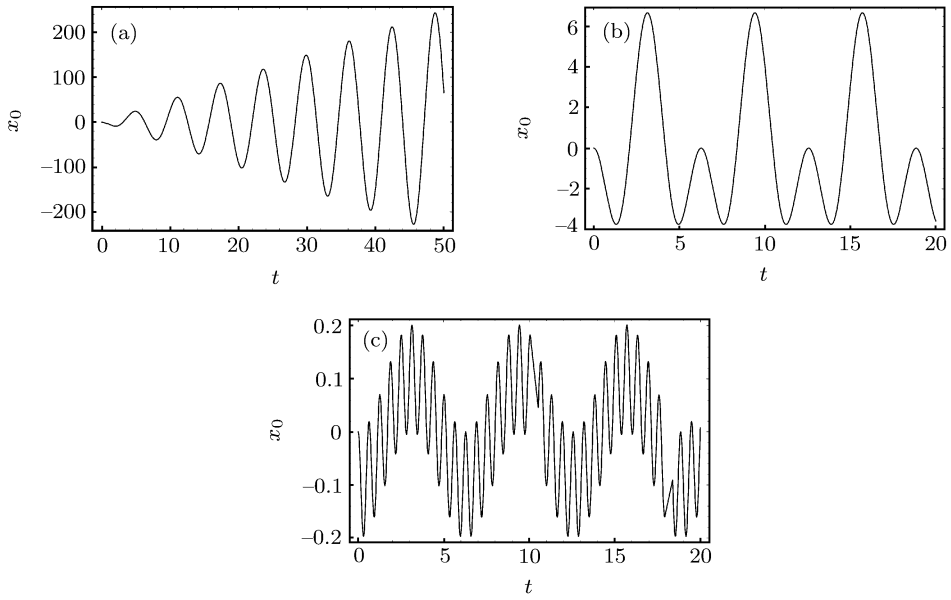


Fig.4. The centre motion of the wavepackets from Eq. (13) for $\varepsilon_0 = 10$, and (a) $\Omega = 1$, (b) $\Omega = 2$, (c) $\Omega = 10$. The space and time variables x_0 and t are in units of $l_{\rm c}$ and $\omega_{\rm c}^{-1}$ respectively.

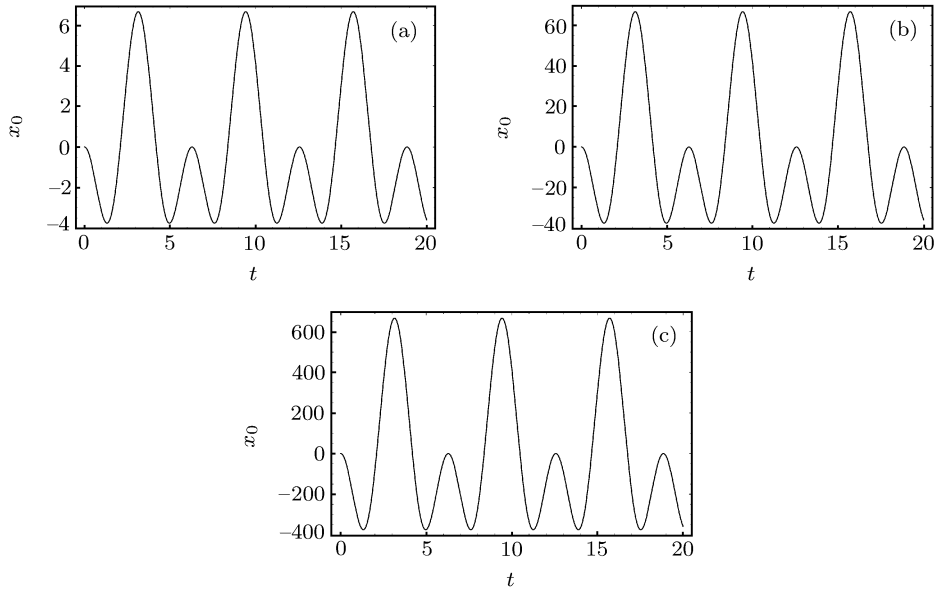


Fig.5. The centre motion of the wavepackets from Eq.(13) for $\Omega = 5$, and (a) $\varepsilon_0 = 10$, (b) $\varepsilon_0 = 100$, (c) $\varepsilon_0 = 1000$. The same units are adopted as those in Fig.4.

From Eqs.(4), (8), (11) and (12) we can acquire the total probability density as

$$|\psi_{n_{\rm c},n_{\rm r}}(x_{\rm c},x_{\rm r},t)|^2 = \frac{\sqrt{c_0}}{\sqrt{\pi}2^{n_{\rm c}}n_{\rm c}!\rho(t)}H_{n_{\rm c}}^2(\xi)\exp(-\xi^2) \times \frac{1}{\sqrt{\pi}2^{n_{\rm r}}n_{\rm r}!}{\rm e}^{-l_{\rm r}^2x_{\rm r}^2}H_{n_{\rm r}}^2(l_{\rm r}x_{\rm r}), \quad n_{\rm c},n_{\rm r}=0,1,2,\ldots. \tag{24}$$

For simplicity, we take parameter set $b_0' = b_0'' = 0$, $\alpha = 0$, $\beta = -\pi/2$, A=B=1, $c_0 = 1$, $\rho = 1$, and $\theta = t$. From Eq.(11) we obtain $\xi = x_{\rm c} - (\varepsilon_0 \cos t \int \cos \Omega t \sin t {\rm d}t - \varepsilon_0 \sin t \int \cos \Omega t \cos t {\rm d}t)$. By applying it to Eq.(24) we plot the spacial distributions of the probability density for different external field frequencies and strengths at several different times.

In Fig.6 we illustrate the translations of the probability wavepackets with the parameters $\varepsilon_0 = 20\sqrt{2}$, $\Omega = 1$, $n_{\rm r} = 2$, $n_{\rm c} = 4$ at three different times, which exhibit the patterns containing three rows and five

columns of the wavepackets. Figure 7 shows the spacial distributions of wavepacket trains $|\psi_{5,1}|^2$ for the different external field parameters at $t = \frac{\pi}{4}$. A comparison between the numerical results in Fig.7 shows

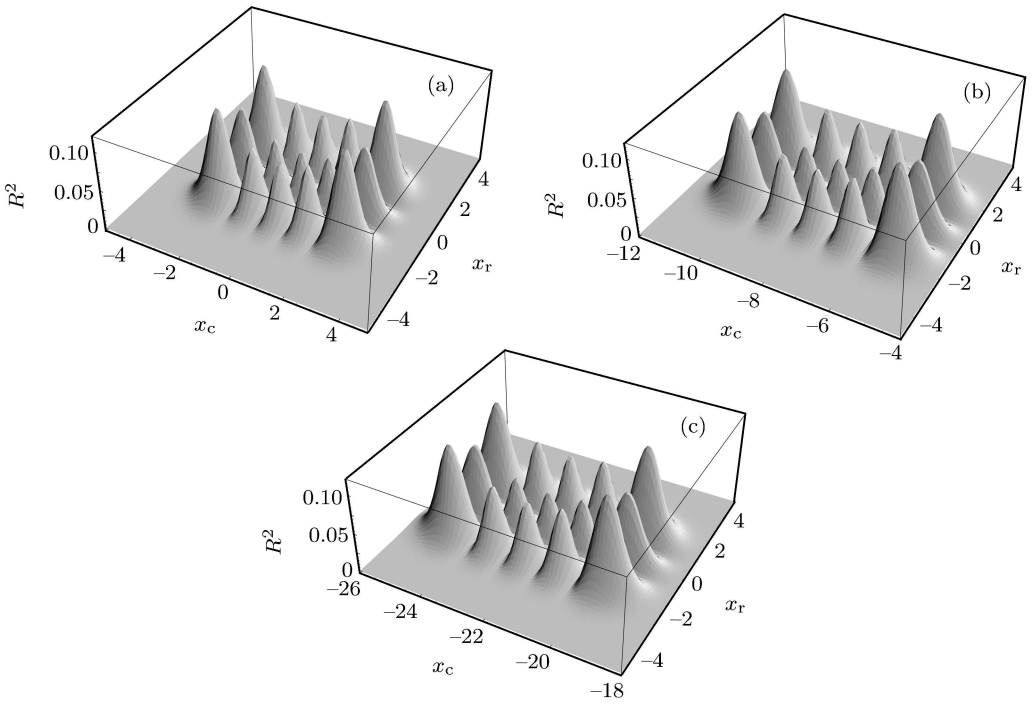


Fig.6. The wavepacket trains of probability density $|\psi_{n_c,n_r}|^2$ versus t from Eq.(24) for $\varepsilon_0 = 20\sqrt{2}$, $\Omega = 1$, $n_c = 4$, $n_r = 2$, and (a) $t = 0$ (b) $t = \pi/4$ (c) $t = \pi/2$. The space and time variables x_c, x_r and t are in units of l_c, l_r and ω_c^{-1} respectively, and the probability density is normalized by l_c^{-1}.

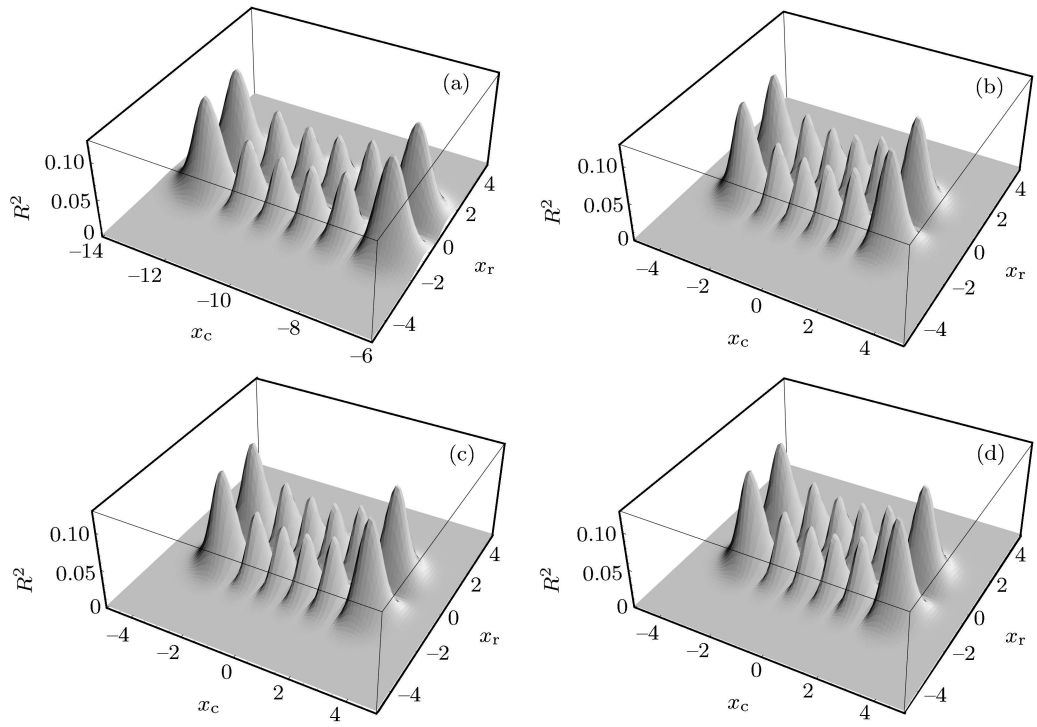


Fig.7. The wavepacket trains of probability density $|\psi_{n_c,n_r}|^2$ from Eq.(24) for $t = \pi/4$, $n_c = 5$, $n_r = 1$, and (a) $\varepsilon_0 = 25\sqrt{2}$ and $\Omega = 1$, (b) $\varepsilon_0 = 25\sqrt{2}$ and $\Omega = 10$, (c) $\varepsilon_0 = 25\sqrt{2}$ and $\Omega = 100$, (d) $\varepsilon_0 = 10\sqrt{2}$ and $\Omega = 100$. The same units as those in Fig.6 are adopted.

that in any case, the relative motion is unrelated to the external field. The numbers of the wavepackets of the relative motion and centre-of-mass motion are determined by n_c and n_r respectively, because of the relative motion being independent of the centre-of-mass motion. From Fig.7 we can also see that variation in laser frequency can cause the change in spacial position of probability wave-packet-train in the low-frequency case, although this operation cannot change the amplitude of wave-packet-train. In the high-frequency case (see Figs.7(b), 7(c) and 7(d)), we can see that the effects of the laser frequency and intensity on the wavepacket are very small. Similarly, Fig.6(b) and Fig.7(a) indicate that with the increase of the laser strength ε_0, the probability wave-packet-trains also displace toward the left in the case of the low-frequency. These results demonstrate that the external field can be used to well control the motion of the wave-packet-trains theoretically. The controlling of the positions of wavepackets and the stability of quantum states are useful for the quantum logic operations based on the trapped ions.[5,43]

5. Discussion and conclusions

In the pseudopotential approximation and large detuning condition, we have studied the exact quantum motions, including the relative motion and centre-of-mass motion, for two trapped ions stored in a Paul trap and subjected to a periodic external field. The external potential generated by a strong laser field resides in a time-periodic linear potential, through the Kramers–Henneberger transformation.[34,35] The same form of the external potential can be obtained approximately from a laser standing wave with variable amplitude in the Lamb-Dicke regime.[1] In order to avoid the coupling between the internal and external states, not only the large detuning between the electronic transition frequency and the laser frequency is necessary, but also the laser strength must be set to be less than the critical value of multiphoton ionization.[44] These can be easily realized for the ions in the internal ground state initially.

Although much work has been done on a two-ion system, the interaction considered in our case is brand-new, which gives rise to some new results as follows. We find that in the above-mentioned approximation and conditions the relative motion is independent of the laser field, but the centre-of-mass motion is closely related to the laser field. We obtain some interesting physical properties from our exact quantum states, such as the expectation energy composed of classical and quantum parts, the generalized squeezed coherent property, and the expectation values of the centre-of-mass position and momentum that reveal good classical-quantum correspondence. The quantum transitions between different centre-of-mass states are investigated by using our exact solutions. The transition probabilities are calculated exactly that approximately agree with the corresponding results obtained by using the Green's function technique.[14] The average energies in the transiting process are illustrated for the resonance and nonresonance cases, and the resonance ladders are found, which depend on the laser strength and interaction time. The results hint us how to control the resonance transitions accurately and timely. Finally, we discuss how to realize the control of the stability and the centre position of the wave-packet-train theoretically by adjusting the external field parameters. Of course, we discuss only some cases of the special parameters, we need to further investigate the unknown information supplied by the exact quantum states, and to seek their possible applications.

Appendix: derivation of the exact solution

Following Ref.[36], we set the test-solution of Eq.(9) as

$$\begin{aligned}\psi_n =& a_n(t)H_n(\xi)\exp[b(t)x_c - c(t)x_c^2 - f^2(t)/2],\\ \xi =& e(t)x_c - f(t).\end{aligned} \tag{A1}$$

Here, $a_n(t), b(t)$ and $c(t)$ are complex functions of time and $e(t)$ and $f(t)$ are real functions. By directly using Eq.(A1), we have the calculations

$$
\begin{aligned}
\mathrm{i}\frac{\partial\psi_n}{\partial t} =& \mathrm{i}a_n\left[\frac{\dot{a_n}}{a_n}H_n + (\dot{e}x_\mathrm{c} - \dot{f})\frac{\partial H_n}{\partial\xi} + (\dot{b}x_\mathrm{c} - \dot{c}x_\mathrm{c}^2 - f\dot{f})H_n\right]\mathrm{e}^{[bx_\mathrm{c}-cx_\mathrm{c}^2-f^2/2]},\\
\frac{\partial\psi_n}{\partial x_\mathrm{c}} =& a_n\left[e\frac{\partial H_n}{\partial\xi} + (b-2cx_\mathrm{c})H_n\right]\mathrm{e}^{[bx_\mathrm{c}-cx_\mathrm{c}^2-f^2/2]},\\
\frac{\partial^2\psi_n}{\partial x_\mathrm{c}^2} =& a_n\left[e^2\frac{\partial^2 H_n}{\partial\xi^2} + (2b-4cx_\mathrm{c})e\frac{\partial H_n}{\partial\xi} + (b^2-2c-4bcx_\mathrm{c}+4c^2x_\mathrm{c}^2)H_n\right]\mathrm{e}^{[bx_\mathrm{c}-cx_\mathrm{c}^2-f^2/2]}.
\end{aligned}
\tag{A2}
$$

Inserting them into Eq.(9) yields

$$
\begin{aligned}
&\mathrm{e}^2\frac{\partial^2 H_n}{\partial\xi^2} + 2(be - \mathrm{i}\dot{f} + \mathrm{i}\dot{e}x_\mathrm{c} - 2cex_\mathrm{c})\frac{H_n}{\partial\xi} + 2\left[\mathrm{i}\frac{\dot{a_n}}{a_n} - \mathrm{i}f\dot{f} + \frac{b^2}{2} - c\right.\\
&\left.+ (\mathrm{i}\dot{b} - 2bc - \varepsilon_0\cos\Omega t)x_\mathrm{c} + (4c^2 - 2\mathrm{i}\dot{c} - 1)x_\mathrm{c}^2\right]H_n = 0.
\end{aligned}
\tag{A3}
$$

Noticing the Hermitian equation $\partial^2 H_n/\partial\xi^2 - 2\xi\partial H_n/\partial\xi + 2nH_n = 0$, Eq.(A3) implies

$$
\begin{aligned}
&\mathrm{i}\dot{c} = 2c^2 - \frac{1}{2},\quad \mathrm{i}\dot{b} = 2bc + \varepsilon_0\cos\Omega t,\quad \mathrm{i}\dot{e} = 2ce - \mathrm{e}^3,\\
&\mathrm{i}\dot{f} = be - \mathrm{e}^2 f,\quad \mathrm{i}\dot{a_n}/a_n = \mathrm{i}f\dot{f} - b^2/2 + c + n\mathrm{e}^2.
\end{aligned}
\tag{A4}
$$

The first expressions in Eq.(A4) is a complex Riccati equation, which can be changed into a complex equation of a classical harmonic oscillator. Through the function transformation $c = \dot{\varphi}/(2\mathrm{i}\varphi)$, we have

$$
\mathrm{i}\dot{c} = \frac{\ddot{\varphi}}{2\varphi} - \frac{\dot{\varphi}^2}{2\varphi^2},\quad 2c^2 = \frac{\dot{-\varphi}^2}{2\varphi^2}.
\tag{A5}
$$

Inserting them into the first expressions in Eq.(A4) yields

$$
\ddot{\varphi} = -\varphi.
\tag{A6}
$$

Setting the real and imaginary parts of φ as φ_1 and φ_2, respectively, they satisfy the same equation (A6), thus they have similar general solutions

$$
\varphi_1 = A\cos(t+\alpha),\quad \varphi_2 = B\cos(t+\beta),
\tag{A7}
$$

where A and B, and α and β are some real constants associated with the initial conditions. In order to keep φ_1 and φ_2 independent of each other, we need $\alpha \neq \beta$ at any case. Given the real and imaginary parts of φ_i, we arrive at the solution

$$
\begin{aligned}
\varphi =& \varphi_1 + \mathrm{i}\varphi_2 = \rho(t)\mathrm{e}^{\mathrm{i}\theta(t)},\\
\rho(t) =& \sqrt{\varphi_1^2 + \varphi_2^2},\quad \theta(t) = \arctan\frac{\varphi_2}{\varphi_1}.
\end{aligned}
\tag{A8}
$$

Real functions $\rho(t)$ and $\theta(t)$ will be used as the known functions in the following calculation.

Returning to the transformation between φ and c yields

$$
c = \frac{\dot{\varphi}}{2\mathrm{i}\varphi} = \frac{1}{2}\dot{\theta} - \mathrm{i}\frac{\dot{\rho}}{2\rho}.
\tag{A9}
$$

Substituting Eq.(A8) into Eq.(A6) yields equations for the phase $\theta(t)$ and module $\rho(t)$

$$
\ddot{\theta} = -2\dot{\theta}\dot{\rho}/\rho,\quad \ddot{\rho} = \rho\dot{\theta}^2 - \rho.
\tag{A10}
$$

Solving Eq.(A10) produces the first integrations

$$
\begin{aligned}
&c_0 = \rho^2\dot{\theta} = \varphi_1\dot{\varphi}_2 - \varphi_2\dot{\varphi}_1 = AB\sin(\alpha-\beta),\\
&c_1 = (\dot{\rho}^2 + c_0^2/\rho^2 + \rho^2)/2.
\end{aligned}
\tag{A11}
$$

Combining Eqs.(A4) with Eq.(A9), and applying the relations (A11), we can easily obtain

$$
\begin{aligned}
b =& \frac{1}{\rho \mathrm{e}^{\mathrm{i}\theta}}\left(\int -\mathrm{i}\varepsilon_0 \cos \Omega t \rho \mathrm{e}^{\mathrm{i}\theta}\mathrm{d}t + b_0' + \mathrm{i}b_0''\right) = b'(t) + \mathrm{i}b''(t),\\
b'(t) =& \frac{b_0'' \sin\theta}{\rho} + \frac{b_0' \cos\theta}{\rho} - \frac{\varepsilon_0 \sin\theta}{\rho}\int \cos \Omega t \rho \cos\theta \mathrm{d}t + \frac{\varepsilon_0 \cos\theta}{\rho}\int \cos \Omega t \rho \sin\theta \mathrm{d}t,\\
b''(t) =& \frac{b_0'' \cos\theta}{\rho} - \frac{b_0' \sin\theta}{\rho} - \frac{\varepsilon_0 \cos\theta}{\rho}\int \cos \Omega t \rho \cos\theta \mathrm{d}t - \frac{\varepsilon_0 \sin\theta}{\rho}\int \cos \Omega t \rho \sin\theta \mathrm{d}t,\\
e =& \frac{\sqrt{c_0}}{\rho} = \sqrt{\dot{\theta}}, \quad f = \frac{b'}{e} = \frac{b'\rho}{\sqrt{c_0}},\\
a_n =& \frac{A_0}{\sqrt{\rho}}\mathrm{e}^{\mathrm{i}}\left[\int\left(\frac{b'^2}{2} - \frac{b''^2}{2}\right)\mathrm{d}t - \left(\frac{1}{2} + n\right)\theta\right].
\end{aligned} \tag{A12}
$$

Here b_0', b_0'' and A_0 are arbitrary integration constants. It is worth noting that $\rho(t)$ and $\theta(t)$ do not depend on the external potential, and only b' and b'' are determined by the external potential. Inserting these into Eq.(A3) leads to the exact solution $\psi_n(x_\mathrm{c}, t)$, and the normalization condition $\int |\psi_n|^2 dx_\mathrm{c} = A_0^2\sqrt{c_0^{-1}}\int H_n^2(\xi)\exp(-\xi^2)\mathrm{d}\xi = A_0^2\sqrt{c_0^{-1}\pi}2^n n! = 1$ gives the constant

$$
A_0 = [\sqrt{c_0}/(\sqrt{\pi}2^n n!)]^{1/2}. \tag{A13}
$$

References

[1] Leibfried D, Blatt R H, Monroe C and Wineland D 2003 *Rev. Mod. Phys* **75** 281

[2] Protsenko I E, Reymond G, Scholosser N and Grangier P 2002 *Phys. Rev.* A **66** 062306

[3] Sasura M and Buzek V 2001 *Phys. Rev.* A **64** 012305

[4] Pachos J and Walther H 2002 *Phys. Rev. Lett* **89** 187903

[5] Poyatos J F, Cirac J L and Zoller P 1998 *Phys. Rev. Lett.* **81** 1322

[6] Jonathan D, Plenio M B and Knight P L 2000 *Phys. Rev.* A **62** 042307

[7] Stenae A, Roons C F, Stevens D, Leibfried D, Schmidt-Kaler F and Blatt R H 2000 *Phys. Rev.* A **62** 042305

[8] Wu Y 2001 *Phys. Rev.* A **63** 052303
Wu Y and Yang X 1997 *Phys. Rev. Lett.* **78** 3086

[9] Nägerl H C, Leibfried D, Rohde H, Thalhammer G, Eschner J, Schmidit-Kaler F and Blatt R H 1999 *Phys. Rev.* A **31** 2991

[10] Feng M and Wang X G 2002 *J. OPT. B: Quantum Semiclass. Opt.* **4** 283
Feng M, Luo X, Zhu X, Shi L and Yan M 1998 *Acta Phys. Sin.* (Overseas) **7** 8

[11] Zeng H and Kuang L 2000 *Commun. Theor. Phys.* **33** 11

[12] Liu X and Fang M F 2002 *Chin. Phys.* **11** 113

[13] Zheng S B 2004 *Chin. Phys.* **13** 61
Zheng S B 2004 *Chin. Phys.* **13** 86

[14] Landovitz L F 1975 *Phys. Rev.* A **11** 67

[15] Hai W, Huang S and Gao K 2003 *J. Phys.* B **36** 3055
Cai L, Hai W and Wu Y W 2006 *Commun. Theor. Phys.* **45** 1089
Hai W, Feng M, Zhu X *et al* 2000 *Inter. J. Theor. Phys.* **39** 1405
Wu Y W, Hai W and Cai L 2006 *Acta Phys. Sin.* **55** 583 (in Chinese)

[16] Truscott W S 1993 *Phys. Rev. Lett.* **70** 1900

[17] Li W and Reichl L E 2000 *Phys. Rev.* B **62** 8269

[18] Wagner M 1996 *Phys. Rev. Lett.* **76** 4010

[19] Li F and Hai W 2004 *Acta Phys. Sin.* **53** 1309 (in Chinese)
Lu G, Hai W and Xie Q 2006 *J. Phys.* A **39** 401
Li F, Hai W, Chong G and Xie Q 2004 *Commun. Theor. Phys.* **42** 599

[20] Hai W, Duan Y, Zhu X *et al* 1997 *Acta Phys. Sin.* **46** 2117 (in Chinese)
Hai W, Feng M, Zhu X W, Shi L, Gao K L and Fang X M 1999 *J. Phys.* A **32** 8265
Hai W, Feng M, Zhu X W, Shi L, Gao K L and Fang X M 1998 *J. Phys. A***31** 2991

[21] Feng M, Hai W, Zhu X, Gao K and Shi L 2000 *Chin. Phys.* **10** 250

[22] Jiang Y R, Feng M, Gao K L and Zhu X W 2001 *Chin. Phys.* **9** 0202

[23] Qu Z J, Liu S D and Yang C L 2005 *Acta Phys. Sin.* **3** 1156 (in Chinese)

[24] Munro W J, Milburn G J and Sanders B C 1999 *Phys. Rev.* A **62** 052108

[25] Feng M, Fang X, Duan Y, Zhu X and Shi L 1998 *Phys. Lett.* A **244** 18

[26] Feng M, Hai W, Zhu X, Fang X, Yan M and Shi L 1999 *Phys. Lett.* A **263** 209

[27] Solano E, Milman P, FilhoR L de M and Zagury N 1999 *Phys. Rev.* A **62** 021401

[28] Yin J and Janavainen J 1995 *Phys. Rev.* A **51** 5

[29] Li L X and Guo G C 1999 *Phys. Rev.* A **61** 1
[30] Shi L, Duan Y W, Feng W, Zhu X W and Fang X M, 1998 *Acta Phys. Sin.* **47** 1248 (in Chinese)
[31] Wagner M 1996 *Phys. Rev. Lett.* **76** 4010
[32] Vorobeichik I and Moiseyev N 1999 *Phys. Rev.* A **59** 1699
[33] Chong G, Hai W and Xie Q 2005 *Chin. Phys.* **14** 1784
[34] Henneberger W C 1968 *Phys. Rev. Lett.* **21** 838
[35] Kramers H A 1938 *Nuovo Cimento* **15** 167
[36] Hai W, Lee C and Chong G 2004 *Phys. Rev.* A **70** 053621
Hai W, Lee C and Chong G 2005 *Phys. Rev.* A **72** 012116
[37] Zeng J 2000 *Quantum Mechanics* 3rd edition (Beijing: Science Press)
[38] Schrade G, Man'ko V I, Schleich W P and Glauber R J 1995 *Quantum Semiclass. Opt.* **7** 307
[39] Ramon G, Brif C and Mann A 1998 *Phys. Rev.* A **58** 2506
[40] Aliaga J, Crespo G and Proto A N 1990 *Phys. Rev.* A **42** 618
[41] Lostelecky V A, Nieto M M and Truax D R 1993 *Phys. Rev.* A **48** 1045
[42] Glück M, Kolovsky A R and Korsch H J 1999 *Phys. Rev. Lett.* **83** 891
[43] Shapiro E A, M Spanner and Ivanov M Y 2003 *Phys. Rev. Lett.* **91** 237901
[44] Gu Y 1996 *Quantum Chaos* (Shanghai Scientific and Technological Education Publishing House) (in Chinese)